

# LOW-REYNOLDS-NUMBER AIRFOILS

*P. B. S. Lissaman*

AeroVironment Inc., Pasadena, California 91107

## INTRODUCTION

The airfoil section is the quintessence of a wing or lifting surface and, as such, occupies a central position in any design discipline relating to fluid mechanics, from animal flight through marine propellers to aircraft. The proper functioning of the airfoil is the prerequisite to the satisfactory performance of the lifting surface itself, and thus the airfoil is of fundamental technical importance.

Transcending functional considerations, the physical shape of the airfoil—teardrop-like or paisley motif-like—seems to have some universal aesthetic appeal. As a consequence, the development and selection of airfoils has exercised an almost mystical fascination on designers. Since the early work of Eiffel and Joukowsky at the turn of the century, fluid dynamicists have recognized the importance of the airfoil shape and have developed a bewildering plethora of airfoil designs and families, many with almost magical claims of efficaciousness. But the ideal shape of an airfoil depends profoundly upon the size and speed of the wing of which it is the core. **This dependence is called *scale effect*.**

In the thirties, the significance of scale effect was first recognized. This relates to the phenomenon that an airfoil that has most excellent qualities on an insect or bird may not exhibit these advantages when scaled up for an airplane wing, and vice versa. Different sizes of airfoils require different shapes. This scale effect is characterized by the chord Reynolds number,  $R$ , defined by  $R = Vc/\nu$ , where  $V$  is the flight speed,  $c$  is the chord, and  $\nu$  is the kinematic viscosity of the fluid in which the airfoil is operating. The Reynolds number quantifies the relative importance of the inertial (fluid momentum) effects on the airfoil behavior, compared

with the viscous (fluid stickiness) effects. It is the latter effects that essentially control the airfoil performance since they dictate the drag or streamwise resistance as well as limiting and controlling the maximum lift of the airfoil. Normally, these qualities are described by the lift and drag coefficients,  $C_L$  and  $C_D$ , defined as  $L/qc$  and  $D/qc$ , respectively, where  $L$  and  $D$  are the lift and drag per unit span,  $q$  is the flow dynamic pressure, and  $c$  is the airfoil chord. The lift and drag coefficients depend on the Reynolds number as well as on the angle of attack of the airfoil, which represents its geometric inclination to the incoming flow.

It is interesting to describe the different wing systems occurring in the wide range of Reynolds numbers over which airfoils are used. We briefly outline the various flight vehicles that are discussed in more detail in an outstanding paper by Carmichael (1981). We draw special attention to Carmichael's encyclopedic report that for the first time puts together all the known theoretical and experimental results, gives the highlight conclusions, and provides the most exhaustive set of references available.

Figure 1 shows this huge scale range, which spans the Reynolds numbers from  $10^2$  to  $10^9$ . Below the lower limit, viscous effects are dominant and it is unlikely that any airfoil-like performance can occur. In the next range, up to  $10^4$ , we find the insects and small model airplanes. Here, the flow is characteristically strongly and persistently laminar. At somewhat higher Reynolds numbers, up to  $10^5$ , one enters the range of flying animals and large model airplanes. Airfoil performance is still relatively low in this range, but a significant improvement in performance occurs as we enter the next regime

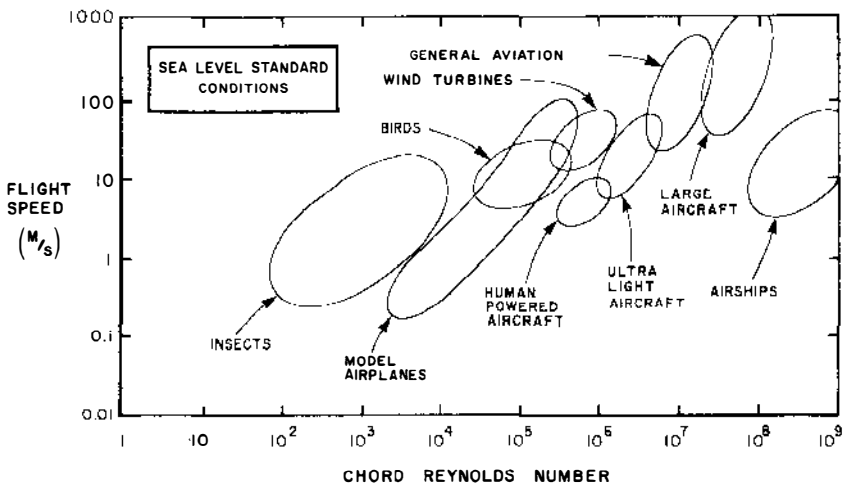


Figure 1 Flight Reynolds-number spectrum.

In this regime, up to about  $10^6$ , we find a major improvement in airfoil performance and the coexistence of a number of fascinating flight systems. We cannot do better here than by quoting Carmichael (1981) directly: "In this regime, we find man and nature together in flight. Large soaring birds of quite remarkable performance, large radio-controlled model aircraft, foot-launched ultralight, man-carrying hang-gliders, and that superb engineering triumph, the human-powered aircraft." Here, we also find the airfoils for smaller modern wind turbines.

Beyond this range, we find sailplanes, light aircraft, and jet transports operating at Reynolds numbers up to and beyond  $10^7$ . In this extensively studied range, some of the highest-performance airfoils have been developed. At high Reynolds numbers, in the neighborhood of  $10^8$ , we enter the regime of large water-immersed vehicles, such as tankers and large nuclear submarines.

The air vehicles described have all been assumed to operate at sea level. Recently, there have been developments in small remotely piloted vehicles (RPVs) used for surveillance, sampling, and monitoring in both military and scientific roles. These vehicles are generally small and often operate at very high altitudes, where the kinematic viscosity is significantly increased by the very low ambient density. These vehicles are not shown in the figure. Because of the extreme operating range, from sea level to 30 km, they span a large Reynolds-number spectrum. Frequently, both the propellers and wings of these RPVs will be required to perform at Reynolds numbers significantly below half a million. This introduces for the first time an aerospace technological requirement for low-Reynolds-number airfoils.

Usually the function of the airfoil is to produce lift, or a force approximately at right angles to its direction of relative motion, while the drag is connected with the forces necessary to propel the lifting surface. Thus, a convenient parameter to measure the effectiveness of an airfoil is its lift-to-drag ratio,  $C_L/C_D$ ; the maximum value of this quantity gives a good indication of the airfoil effectiveness. For design purposes, it is desirable that this maximum occur at a high lift coefficient so that the physical size of the lifting surface is minimized. An indication of the magnitude of this lift is given by the performance parameter,  $C_L^{3/2}/C_D$ , which gives somewhat more weighting to the lift coefficient. For detailed design of lifting surfaces, it is necessary to know even more of the performance structure of the airfoil—that is, how the lift and drag vary with angle of attack at a given Reynolds number, the airfoil signature, expressed by its lift-to-drag polar.

We have alluded to the fact that at lower Reynolds numbers the viscous effects are relatively large, causing high drags and limiting the

maximum lift, while at the higher values the lift-to-drag ratio improves. There is a critical Reynolds number of about 70,000 at which this performance transition takes place. This dramatic improvement can be seen most vividly in Figure 2, taken from McMasters & Henderson (1980). Here we note the striking change in performance for smooth airfoils near the critical Reynolds number where the lift-to-drag ratio increases more than an order of magnitude. It is of great interest that a rough or turbulated airfoil does not exhibit this abrupt performance change with Reynolds number. We note from Figure 2 that this critical Reynolds number really divides the airfoils of the insect class (less than  $10^4$ ) from those of the large airplane class (above  $10^6$ ).

Some representative airfoil sections of this transitional range are shown in Figure 3. At the low end, we have the insects, with the interesting feature that it is not necessary to have a smooth surface; in fact, it is likely that the discontinuities are desirable to delay flow separation. For birds, however, smoothness begins to be important, as shown by the pigeon section. In the middle range is the Eppler 193, an airfoil with excellent performance at a Reynolds number of about 100,000, and at the high end, the Lissaman 7769, the airfoil used on the *Gossamer Condor* and *Albatross*, and the Liebeck L 1003, an airfoil of striking performance that provided clues on which the design of the Lissaman 7769 was based.

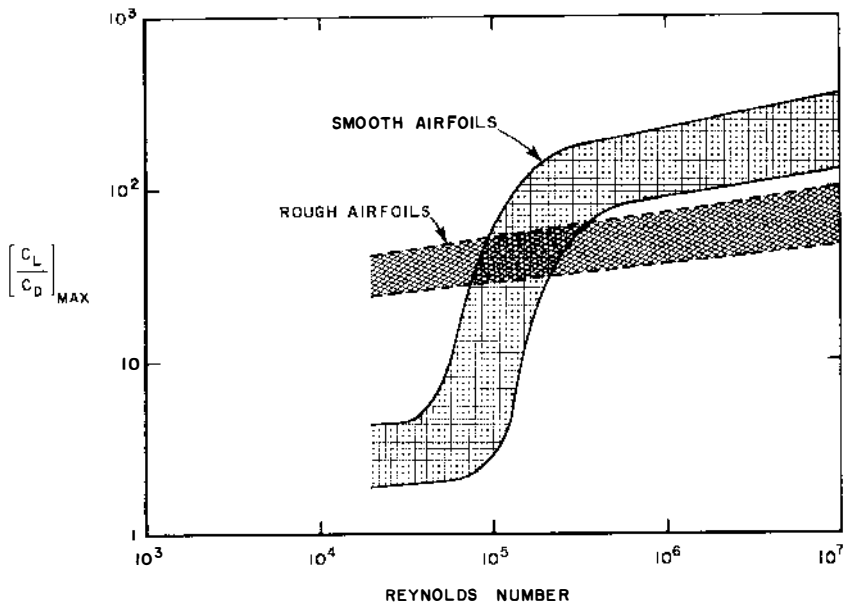


Figure 2 Low-Reynolds-number airfoil performance.

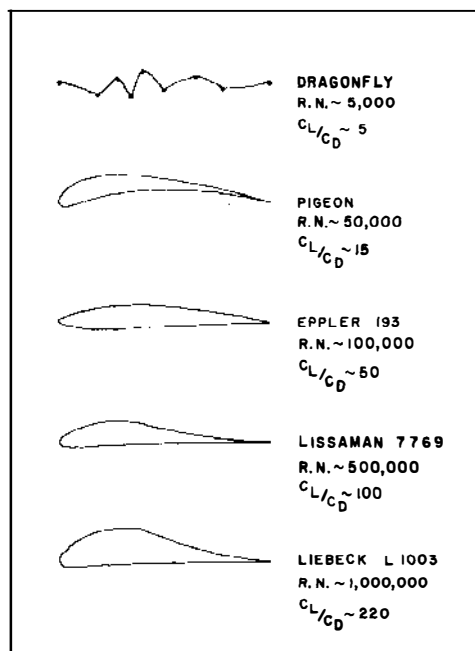


Figure 3 Representative low-Reynolds-number airfoils.

The 7769 airfoil (Lissaman 1980) was developed especially for human-powered airplanes. The design requirements were that the airfoil should have low drag, relatively high lift, a mainly flat undersurface (it is linear for the last 80%), and that it should be tolerant to irregularities due to low-fidelity construction and distortion of covering surface in flight. The latter two requirements, apparently whimsical in the world of high technology, proved to be critically important in the milieu in which the Gossamer aircraft were built, flown, crashed, and repaired.

In the following discussion, we describe the fluid mechanics, performance, and design of low-Reynolds-number airfoils, which we take to include the range between Reynolds numbers of about  $10^4$  and  $10^6$ . We do not discuss compressibility effects, although these do occur at high altitudes on RPVs, and we confine the discussion to two-dimensional flows, although the third dimension is important on fans, propellers, and low-aspect-ratio wings.

## FUNDAMENTAL FLUID MECHANICS

All airfoils have regions of lower-than-static pressure. Normally, these are most pronounced on the suction (or lifting) surface; however, the

effects of thickness itself on a symmetrical nonlifting airfoil will introduce a region of accelerated flow and the associated lower pressure. The higher speed flow must then return to approximately free-stream conditions at the trailing edge, experiencing a pressure recovery through an adverse pressure gradient. For airfoils operating in excess of  $10^6$  Reynolds number, this adverse gradient normally occurs after transition so that it is impressed on a turbulent boundary layer that can negotiate quite severe adverse pressure gradients without separation. However, in lower Reynolds-number ranges, the boundary layer at the onset of the pressure rise may still be laminar, and thus unable to withstand any significant adverse pressure gradients. The performance of low-Reynolds-number airfoils is entirely dictated by the relatively poor separation resistance of the laminar boundary layer.

In the lowest Reynolds-number range (below 30,000), conditions are normally such that the boundary layer is still laminar beyond the point at which pressure recovery commences and, provided the pressure gradient is mild, complete laminar flow can occur for small angles of attack. As the lift is increased, the adverse gradients become more severe and laminar separation occurs, limiting the lift coefficient and significantly increasing the drag. At the lowest Reynolds number, this separation may occur over the entire rear of the airfoil, extending into the wake. However, when a laminar boundary layer separates, the separated layer very rapidly undergoes transition to a turbulent flow, because of the increased transition susceptibility of the separated shear layer. The increased entrainment of this turbulent flow makes it possible for the flow to reattach as a turbulent boundary layer. This forms what is called a *laminar separation bubble*.

Figure 4 shows the general geometric structure of a laminar bubble. After laminar separation, the flow proceeds at an approximately constant separation angle and the processes of transition occur. As turbulence develops, the increased entrainment causes reattachment. After reattachment, the turbulent boundary layer reorganizes itself to form an approximately normal turbulent profile.

These bubbles exhibit a very interesting spectrum of behavior and have been extensively studied, with particular reference to the conditions of reattachment and the length of the bubble. It has been pointed out by Carmichael (1981) that a rough rule is that the distance from separation to reattachment can be expressed as a Reynolds number based on bubble length of approximately 50,000. Thus, for airfoils of chord Reynolds number of about this magnitude, the airfoil is physically too short for reattachment to occur. This accounts for the general observation that the critical Reynolds number of an airfoil is about 70,000. Below this value it is unusual for reattachment to occur.

For airfoils at a Reynolds number higher than 70,000, conditions can exist for reattachment so that a laminar bubble can form. Depending upon the airfoil shape, different types of laminar bubbles occur, characterized by the bubble length as either short or long.

Being a boundary-layer effect, bubble geometry must properly be described in scales of boundary-layer heights, which can be normalized and nondimensionalized by forming a local Reynolds number using length scales from the bubble. The pressure gradients, on the other hand, scale principally with the airfoil shape and chord. However, for the airfoil designer, it is useful to give typical bubble proportions in terms of the airfoil chord. It must be noted that such proportions are strongly Reynolds-number-dependent.

At a Reynolds number of about  $10^5$ , the long bubble generally extends over 20–30% of the airfoil and significantly changes the pressure distribution by effectively altering the shape over which the outer potential stream flows. At higher Reynolds numbers, a short bubble may form. The short bubble is generally of length of the order of a few percent of the airfoil chord and thus does not greatly alter the pressure from its normal attached distribution. So the short bubble, initially, generally represents the transition-forcing mechanism, and as long as it stays short, it does not greatly affect the airfoil performance. However, as the angle of attack increases, requiring a greater pressure recovery in the laminar bubble for reattachment, the short bubble can “burst” to form a long

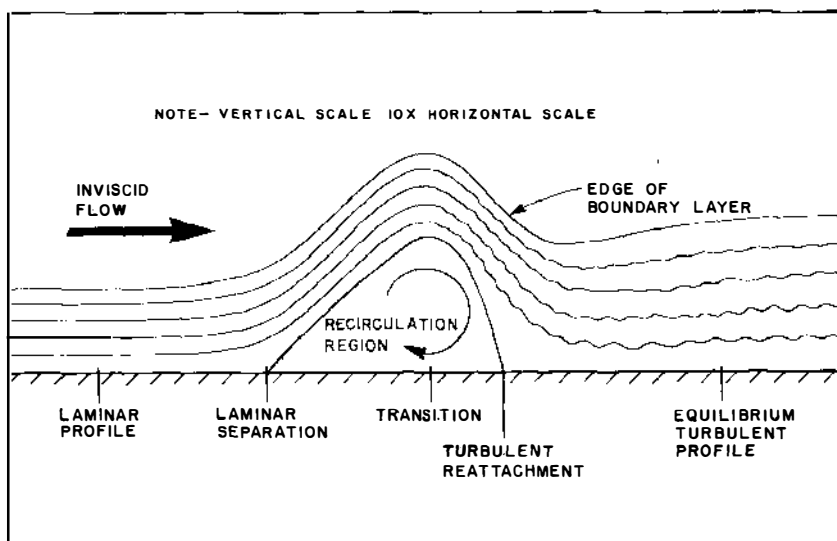


Figure 4 Structure of laminar separation bubble.

bubble. This bursting causes an abrupt stall and sudden severe deterioration in airfoil performance.

As might be expected, the stability of the short bubble is marginal and its bursting can be triggered by many extraneous flow effects. Frequently after bubble burst, reducing the angle of attack will not immediately "unburst" the bubble, so that hysteresis effects occur as the angle of attack is cycled. It is this behavior of short- and long-bubble formation, and bursting with angle of attack and Reynolds number, that causes such striking differences in performance of various airfoil shapes. Carmichael (1981) gives an extensive discussion of the variety of polar shapes that can occur because of these effects and classifies them into five basic characteristic modes.

Figure 5 illustrates the two most distinct of these modes on two different airfoils at a Reynolds number of 50,000. Note that both airfoils have the same minimum drag and  $(C_L/C_D)_{\max}$ . The well-behaved polar is similar to that of conventional airfoils at Reynolds numbers above 1,000,000; the other polar represents the gyrations that can occur in the critical Reynolds-number range. Figure 5 demonstrates the importance of considering the airfoil polar as well as its maxima and minima in lift and drag.

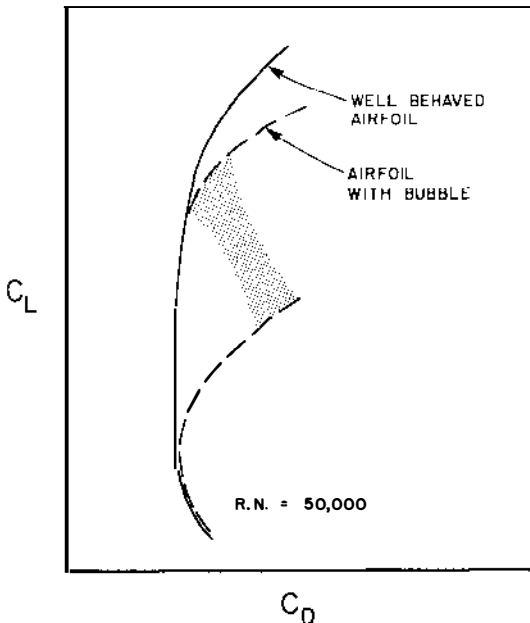


Figure 5 Effect of laminar bubble on lift-drag polar.



As the Reynolds number of the airfoil increases and approaches 200,000, it becomes more likely that the laminar bubble can be avoided, since it is usually possible to design the airfoil so that transition occurs upstream of any severe adverse pressure gradient. Now, the pressure recovery occurs in the turbulent boundary layer, with its much greater resistance to separation. However, it is still apparent that performance is less than would occur at a higher Reynolds number, principally because the separation resistance of the turbulent boundary layer increases as the Reynolds number becomes larger.

Above a Reynolds number of 500,000 there is a further improvement in airfoil characteristics. There is an extensive body of literature available on this regime. The laminar bubble can still occur in injudicious designs but can usually be avoided. It is noted that the laminar bubble is not strictly associated with the chord Reynolds number but, rather, with the local boundary-layer Reynolds number at which pressure recovery first commences. If this recovery is very near the leading edge of the airfoil and the adverse gradients are severe, bubble-type behavior may again develop. Such a situation occurs with thin airfoils of small nose radius at high angle of attack, even at Reynolds numbers exceeding a few million.

Further performance improvements occur for airfoils operating above the 1,000,000 Reynolds number range, although the rate of increase is generally slow and advantages are painfully won. Laminar separation should not be a problem here and the advantages occur through the weak reduction in turbulent skin friction as the Reynolds number ( $R$ ) increases. The drag coefficient in this case varies approximately proportionally to  $R^{-1/3}$ . The maximum lift coefficient also increases slowly because of the increased separation resistance of the turbulent boundary layer. Lower limits on drag can readily be estimated; they correspond quite closely to the skin friction of an attached flow with a given transition point. Upper limits on lift have not been as clearly defined; however, a particularly inspired approach was made by Liebeck (1978), who took the point of view that the maximum upper-surface lift would be obtained by developing an upper-surface adverse pressure distribution that was uniformly critically close to separation. On this basis, the entire pressure-recovery region would be operating at its maximum capacity. This involved assuming an incipient separation turbulent profile, calculating the pressure field required to produce this, and deriving the airfoil shape from this critical-velocity distribution. These airfoils caused some surprise by performing in test just as well as, and in some cases better than, the theoretical predictions. It is believed that Liebeck-type airfoils have achieved the best  $(C_L/C_D)_{\max}$  of any tested in the Reynolds number range from about 500,000 to 2,000,000.

The necessity of eliminating laminar separation at lower Reynolds numbers has led to the development of techniques to artificially accelerate transition, or to “turbulate” the boundary layer. A wide variety of techniques are available to accomplish this and they are discussed in detail by Carmichael (1981). Transition-promoting devices, called *turbulators*, range from simple mechanical roughness elements in the form of serrations, strips, bumps, or ridges near the airfoil leading edge, through transpiration methods using airjets emitted from surface orifices of fractional-percentage chord diameter, to exotic procedures like beaming sound waves of frequencies calculated to cause transition at the wing surface, or mechanically vibrating the wing itself. Transition can also be accelerated by increasing the free-stream turbulence with wires or grids ahead of the airflow. The latter methods sound impractical but are intended to simulate flight conditions in which engine noise, airframe vibration, or strong ambient turbulence introduces such effects.

The design of turbulators is subtle, since the transition-inducing mechanism must be of significant magnitude to produce turbulence and suppress laminar separation without causing the boundary layer to become unnecessarily thick. A thick turbulent boundary layer may again suffer separation, or at least cause an increase in drag. Studies of the effect on  $(C_L/C_D)_{\max}$  with fixed trip strips, typically of about 1/4% of the chord and located in the first 25% of the chord, have been conducted on a number of airfoils. At a Reynolds number of about 40,000, an increase of about 20% in this parameter is noted, while at 60,000 the increase is only about 10%. At a Reynolds number of 100,000, however, no distinct improvement is seen and some of the airfoils tested experience a reduction in lift-to-drag ratio.

## EXPERIMENTAL TESTING OF AIRFOILS

Airfoil testing involves an intrinsic difficulty in that the two quantities to be correlated—the lift and the drag—differ in magnitude by a factor of about 100. In addition, a major region of interest is usually in the vicinity of stall and separation, where small changes can trigger large effects. In wind-tunnel testing, there are frequently difficulties with wall effects. These are both inviscid, where the confined potential flow must be taken into account, and viscous, where boundary layers emanating from the walls or the support system can influence the boundary-layer behavior of the test airfoil section. In addition, it is important to consider the incoming turbulence in the test flow, as well as any perturbations due to mechanical or acoustic disturbances. These disturbances can be partially avoided by free-flight testing (essentially, carefully executed performance

measurements of gliding wings, either in the atmosphere or in a large, closed building). The problems here involve the inevitable three-dimensional nature of the flow as well as the difficulty of isolating the airfoil performance from that of the rest of the glider.

For wind-tunnel testing, it is possible to measure the forces directly or to measure the pressures on the airfoil and the velocity and pressure in the wake. Pressure-measuring techniques have the advantage of providing information on the details of the chordwise pressure distribution. For free-flight testing, the principal observable is the flight trajectory, and great pains must be taken to eliminate unsteady effects either from improper launching or from ambient air-mass motions. Flow visualization is applicable to both test methods and will provide valuable qualitative information, as well as quantitative data on the geometrical features of transition and separation.

For all the above reasons, test data in the low-Reynolds-number range have long been regarded with skepticism, especially earlier test results, and there is indeed a substantial record of nonrepeatability of data from tests in different facilities. Sometimes this is attributable simply to inaccurate measurement techniques, but more frequently it can be because the model and environment are actually different from one test to another; the model shape may not be true (the profound effect of turbulator devices of size less than 1/2% of chord illustrates this point), the tunnel turbulence may be different, or the boundary effects may vary.

Even in modern wind-tunnel test facilities with advanced instrumentation and airflows of turbulence levels lower than 1/10%, striking differences in airfoil performance are reported, particularly near the critical Reynolds number of about 70,000. Carmichael (1981) reports that for a good standard low-Reynolds-number airfoil, the Eppler 61, tests in two facilities gave a  $(C_L/C_D)_{\max}$  of about 50, while a third facility reported about 25 for this value. It is disturbing for the practical designer to note that the high data were inferred by integrating wake flow measurements, while the low performance (25) was obtained by measurement of actual forces on the airfoil, a much more convincing observable if properly executed. This discrepancy may be due to spanwise flow variations.

Modern collections of airfoil test data are given by Miley (1982), Althaus & Wortmann (1981), and Althaus (1980).

## THEORETICAL DESIGN OF AIRFOILS

The analytical design of airfoils has always occupied an important position in aeronautical research. Many low-Reynolds-number airfoil applications involve flows that are essentially two-dimensional and in-

compressible, and are thus particularly amenable to analysis. It has already been noted that at high altitudes, low-Reynolds-number airfoils may indeed operate at high Mach numbers and thus experience compressibility effects, while propellers, fans, and low-aspect-ratio wings operate in strongly three-dimensional flow fields. However, here we consider only two-dimensional incompressible flows, a class that covers a large number of applications. We do not discuss airfoils with separate elements, like slats, vanes, or flaps, confining the discourse to single-element airfoils.

Two-dimensional inviscid-flow theory is a very well developed discipline in fluid mechanics and has been a productive research area since the earliest days, when it was first noted that there are a number of simple conformal transformations that convert the circle into airfoil-like shapes with a rounded, bulbous leading edge and a tapered, wedge, or cusp-like trailing edge. This makes it possible to obtain exact analytical formulations of the flow field about airfoils using complex-variable techniques. The availability of numerical computing machines of high speed and capacity has greatly extended the scope and range of flow calculations for airfoils of arbitrary nonanalytical shapes. Thus, the determination of the potential flow about any shape can now be accomplished with dispatch and precision.

The attached boundary layer on the airfoil can also be calculated with good accuracy, providing the location of transition can be reliably estimated. Thus, assuming that separation does not occur, it appears that methods are now available to reliably compute airfoil performance at low Reynolds numbers. An excellent discussion of a modern viscous-inviscid design procedure is given by McMasters & Henderson (1980).

If the flow is fully attached, then the methods described above can be used to predict both the lift and drag with good accuracy and to examine the effects of changes in the airfoil shape.

However, airfoil performance is always limited by separation. In the high-Reynolds-number situation, this usually takes place in the turbulent boundary layer toward the rear of the airfoil. Methods are available to estimate this separation lift coefficient and even the separated drag, although normally this drag is so high that its precise value is not of great interest. Over the last 50 years, an extensive body of research has developed on the stall of airfoils at Reynolds numbers exceeding 1,000,000, and it is correct to say that the field is well understood to the extent that for regular airfoil shapes one can calculate with high precision the lift and drag of such an airfoil up to the separation and also make satisfactory estimates of the poststall performance.

For large Reynolds numbers, above 1,000,000, transition normally occurs near the minimum pressure point, at the first onset of the adverse pressure gradient. This will normally assure that a separation-resistant turbulent boundary layer occurs in the pressure recovery region. However, if the initial adverse gradient is too severe, a laminar separation occurs, as previously described; transition occurs in the separated region, and although reattachment occurs, the drag of the airfoil increases and the maximum lift is reduced. This effect can be eliminated by delicate contouring of the airfoil near the minimum pressure point to create a less severe adverse pressure gradient, called an *instability range*, to accomplish separation-free transition.

These design techniques encompass both the direct procedure, where for a given airfoil shape the pressure fields are determined, and the inverse procedure, where for a given pressure field the airfoil shape is determined. Historically, the direct methods appear to have developed first. Evidently, these methods require an airfoil shape definition that is presumably arbitrary (or even mystical) and not necessarily optimum. A more satisfying and rational procedure is to derive the airfoil shape by using analytical methods from the required pressure characteristics. A most interesting application of this inverse approach is exemplified by the important research of Liebeck, which began as an attempt to develop airfoils of higher lift than had previously been believed possible. These high-lift designs have been proven in test, and also have been shown to have very desirable low-drag characteristics and performance polars. It is believed that these Liebeck airfoils have developed the highest lift-to-drag ratios of any airfoil at any Reynolds number. These design methods assume attached flow and are acceptable down to a Reynolds number of about 300,000.

In the lower Reynolds-number ranges, unusual performance characteristics develop, all caused in one respect or another by different features of transition, laminar separation, and laminar bubble behavior (described in the previous section). Although a considerable amount of theoretical and experimental work has been done here, there is still no generally accepted method of calculating the development of a laminar bubble or even reliably predicting transition at lower Reynolds numbers. However, empirical results are available to the designer, including a number of relatively simple criteria involving relationships between the appropriate boundary-layer parameters in separated flows. Approaching the problem from the pure fluid-mechanical point of view, recent work has involved attempts to calculate the detailed flow structure in the bubble. These use numerical methods to solve fairly complete expressions of the basic flow

equations, and correlate well with test data. An excellent summary, including the major results of the various papers, is given by Carmichael (1981).

## SPECIAL-PURPOSE AIRFOILS

Airfoil design has progressed through a number of stages. The first consisted of designing families of airfoil shapes on geometrical principles. In some cases, simple analytical shape formulations were intentionally chosen, based on some intuition that such “pure” curves might show magical fluid-mechanical properties. Some members of these families have indeed exhibited admirable characteristics. The next stage involved specifying not the airfoil shape, but the pressure distributions, with various smooth or semi-analytical properties that were generally desirable from lift, transition, and separation aspects. Families of airfoil shapes were then derived to produce these pressure fields. A more sophisticated further stage, exemplified by Liebeck, involved defining the pressure distribution to meet specific high-lift or low-drag requirements while assuring boundary-layer attachment. The airfoil shape was then developed by inverse methods.

The above techniques provide the designer with a compendium of airfoils from which he can choose those which best meet his vehicle requirements. Sometimes the match between the designer specification and the best-fitting performance may leave much to be desired.

Modern computing techniques and an increased understanding and quantification of critical boundary-layer behavior have now made it possible to design airfoils specially tailored for a given flight vehicle, thus assuring the best possible match. Two airfoils designed along these lines are described below, and are shown in Figure 6.

The BoAR 80 (McMasters et al. 1981) was designed for a new ultralight sailplane of 120-kg all-up weight and 11.5-m span. The high-lift requirements dictated the upper-surface shape and defined the maximum lift that could be carried by the suction (upper surface). Additional lift was required and had to be obtained by undercamber on the lower surface to increase the overpressure on that side. Thus, the pressure distribution required to develop this lift without separation was defined, and the airfoil was designed by inverting this pressure field. Then, using direct methods, the high-speed (low lift and angle of attack) pressure distribution was determined. It was estimated that separation would occur near the leading edge on the lower surface, in this case with undesirably high drag. Thus, the full flight-range requirements could not be met by the highly cambered shape required for high lift.



However, the high-speed requirements could be met by maintaining the upper-surface shape and dropping the lower surface to increase the thickness and reduce the camber. This provided an airfoil with separation-free low-drag performance in the high-speed, low-angle-of-attack flight regime. The airfoil is intended to change configuration during flight, activated by command, as one might use a flap.

The BoAR 80 airfoil has not been tested but the design calculations indicate a minimum drag coefficient in the thin configuration of about 0.0065 with a  $(C_L/C_D)_{\max}$  in the cambered configuration of 147.

The Lissaman-Hibbs 8025 airfoil (MacCready et al. 1981) was designed for the *Solar Challenger*, a photovoltaic-powered aircraft of 150-kg all-up weight and 14.3-m wingspan. The aerodynamic requirements called for a maximum lift coefficient of about 1.6 and a gentle stall, with low drag at the cruise lift coefficient. These were not severe. The geometrical requirements, however, were draconian—that the upper surface should be flat over its major length. This is a quite traumatic constraint to the designer, who depends upon smooth-flowing curves to achieve good flow characteristics.

The eminently practical reason for this constraint is that the upper surface of the wing and stabilizer are almost entirely covered with rectangular silicon solar cells, 2×6 cm in size. It is of interest that the stabilizer served not in its titular function but principally as a platform for the photovoltaic system. It was decided that the cells should be on the outer surface of the wing to maximize cooling, and that the solar panels

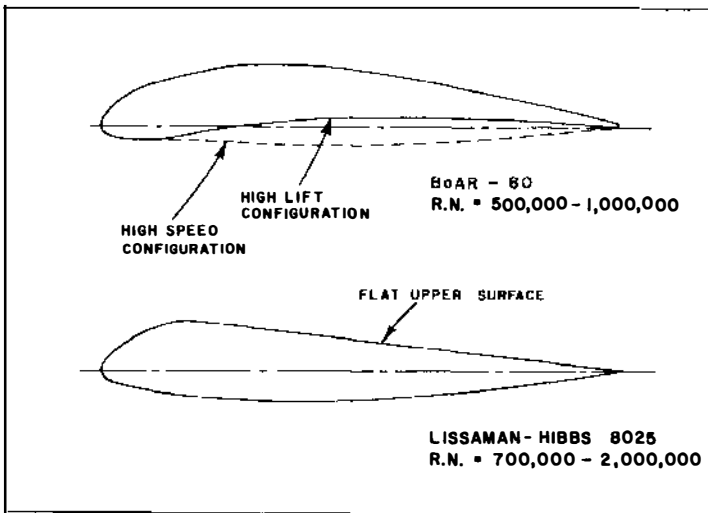


Figure 6 Special purpose low-Reynolds-number airfoils.

should be perfectly flat to simplify installation and also to minimize drag due to unavoidable surface irregularities if a curved surface was approximated by a multifaceted, trapezoidal shape, “tiled” by the cells (each of which was about 1.6% of the airfoil chord). Also, the flat surface exposes all cells to the same sun angle, thus avoiding any voltage unbalances. The airfoil was designed by direct computer methods to cruise with low drag at a lift coefficient of about unity. Desirable features of the pressure distribution on the upper surface could not be obtained by modifying that surface, but had to be achieved by the shape of the nose section and the undersurface.

The flat-topped stabilizer (not shown here) was designed on the same principles, except that since it was mainly a cell platform, its lift coefficient was very low and the design object was to minimize the section drag by achieving the maximum extent of laminar flow on the lower surface. Both airfoils, as finally developed, were perfectly flat for the major portion of the upper surface; the wing for the last 85%, the stabilizer for the last 90%.

No laboratory data are available on these airfoils, which were tested in the ultimate wind tunnel—the sky. In 1981, the *Solar Challenger* flew 350 km from France to England powered only by the sun. Crude flight tests indicate that the minimum drag coefficient of the wing airfoil is about 0.009, while the  $(C_L/C_D)_{\max}$  is about 160.

## PARTING COMMENTS

Low-Reynolds-number airfoils encompass the heart of the lift system of a magnificently wide variety of flying vehicles, from birds and bats to human-powered aircraft and remotely piloted vehicles. There is an extensive body of research on airfoil performance in this range and, at first glance, these data present a bewildering assortment of inconsistencies. However, we now understand the mechanics of the flow well enough to be able to explain this behavior, at least in the sense that for a given performance we can interpret it as a rational consequence of the boundary-layer behavior in the highly sensitive Reynolds-number domain where transition, separation, and reattachment are all occurring in a short length of the airfoil. In other words, if we know the events that happened, we can say why.

The concomitant question of how to make these events happen once it is known why they do is much more difficult and is far from solved. For this reason, the design of low-Reynolds-number airfoils, particularly at Reynolds numbers below 300,000, is still a black art. It is likely, however, that most of the fluid-mechanical processes have been qualitatively



defined, and good progress is being made to place these phenomena on a quantitative predictive basis.

The study of low-Reynolds-number airfoils is an intriguing subject. Its fascination can be attested to by the large volume of excellent amateur, unsupported, or minimally funded research that it has engendered. To date, there have been no critical military or commercial requirements for a systematic airfoil technology in this regime. Nonetheless, an extensive and intelligent body of knowledge exists and expands. Apparently, there are people who study this field simply because they find its challenges elegant and attractive. With the appearance of the new small unmanned aircraft, the RPVs, with their military and scientific importance, it is possible that there will be a surge of adequately funded activity. If this research is directed with a sufficiently long-sighted vision so that the fundamental issues as well as the immediate practical ones are tackled, we may see a resolution of some of the principal unsolved issues. These issues, relating intimately to the great interconnected puzzle of transition, turbulence, separation, and reattachment, are fundamental to classical fluid mechanics.

#### Literature Cited

- Althaus, D. 1980. *Profilpolaren für den Modellflug*. Karlsruhe: NeckarVerlag
- Althaus, D., Wortmann, F. X. 1981. *Stuttgarter Profilkatalog 1*. Braunschweig: Vieweg & Sohn. 320 pp.
- Carmichael, B. H. 1981. Low Reynolds number airfoil survey. Vol. 1. *NASA CR 165803*
- Liebeck, R. H. 1978. Design of subsonic airfoils for high lift. *J. Aircr.* 15:547-61
- Lissaman, P. B. S. 1980. Wings for human-powered flight. *Proc. AIAA Symp. Evol. Aircr. Wing Design*, SP 802, pp. 49-56
- MacCready, P. B., Lissaman, P. B. S., Morgan, W. R., Burke, J. D. 1981. Sun-powered aircraft design. *AIAA Repr. 81-0916*
- McMasters, J. H., Henderson, M. L. 1980. Low speed single element airfoil synthesis. *Tech. Soaring* 6(2):1-21
- McMasters, J. H., Nordvik, R. H., Henderson, M. L., Sandvig, J. H. 1981. Two airfoil sections designed for low Reynolds numbers. *Tech. Soaring* 6(4):2-24
- Miley, S. J. 1982. A catalog of low Reynolds number airfoil data for wind turbine applications. Prepared for Rockwell Int. Corp., Energy Syst. Group, Rocky Flats Plant, Wind Syst. Program